J Mol Model (2012) 18:455–466
DOI 10.1007/s00894-011-1063-y

ORIGINAL PAPER

Geometric distortions on a three-coordinated T1 Cu site model as a potential strategy to modulate redox potential. A theoretical study

Hugo Vázquez-Lima · Patricia Guadarrama · Claudia Martínez-Anaya

Received: 3 August 2010 / Accepted: 22 March 2011 / Published online: 4 May 2011

Abstract A model of the three-coordinated T1 Cu site from *Trametes versicolor* was considered to evaluate the effect on redox potential of geometrical distortions in the copper coordination sphere. Systematic modifications of geometrical parameters (distances and angles) of the coordination sphere of the T1 Cu site were carried out within a density functional theory (DFT) framework, to evaluate their effects on electron affinity directly related to redox potential. The most promising result in terms of redox potential increment was distortion of the dihedral angle $C_{methylthiolate}$–S–Cu–N_{ImA} (ω), which can be rationalized as a decrease in the overlap of imidazole orbitals in the redox-active molecular orbital (β-LUMO). This overlap is minimized when ω achieves the value of 10°, therefore, this conformation might have the highest redox potential. From the molecular orbital viewpoint, a parallelism was found between the effect caused by the presence of a fourth ligand and the distorted three-coordination, which could be extrapolated to spectroscopic properties. It was also found that solvation effects on the redox potentials during geometrical distortions produce a very similar tendency, independently of the polarity of the solvent.

Electronic supplementary material The online version of this article (doi:10.1007/s00894-011-1063-y) contains supplementary material, which is available to authorized users.

H. Vázquez-Lima · P. Guadarrama (✉)
Instituto de Investigaciones en Materiales,
Universidad Nacional Autónoma de México,
Apartado Postal 70–360, CU, Coyoacán,
Mexico DF 04510, Mexico
e-mail: patriciagua@iim.unam.mx

C. Martínez-Anaya
Departamento de Ingeniería Celular y Biocatálisis, Instituto de Biotecnología (IBT), Universidad Nacional Autónoma de México,
Av. Universidad 2001, Col. Chamilpa,
62250 Cuernavaca, Morelos, Mexico

Keywords Density functional theory · Laccase · Redox potential · Enzymatic model

Introduction

Laccases are enzymes belonging to a family known as multicopper oxidases containing four copper atoms classified in three different types (T1, T2, and T3), according to their spectroscopic properties in oxidized state [Cu (II)] [1].

These enzymes have an enormous biotechnological potential in environmental remediation since they are able to catalytically oxidize several harmful substrates such as phenols and aromatic amines. The accepted mechanism involves a first stage where Cu (II) in the T1 Cu site is reduced to Cu (I), and this active site is then re-oxidized with the concomitant reduction of O_2 to H_2O [2]. Nowadays, there is a growing interest in understanding the complex mechanisms involved in the activity of laccases and, at the same time, there is a constant search for new varieties of laccases with higher stability and higher redox potential to cover a wider spectrum of substrates [3].

The T1 Cu, responsible for the blue color of these enzymes when oxidized [4], has been studied extensively, and is a recurrent motif found in proteins involved in redox processes. This copper atom is surrounded by two histidine (His) and one cysteine (Cys) residues, all of which are conserved in all T1 Cu sites. A fourth residue can be methionine (Met), glutamine (Gln), leucine (Leu), isoleucine (Ile) or phenylalanine (Phe), depending on the protein.

In most proteins, the T1 Cu site is directly responsible for the redox potential, which is modulated by five factors: (1) the number of copper coordinated residues [lower coordination numbers of Cu (II) destabilized this state, resulting in higher redox potentials], (2) distortions in the

copper coordination sphere, (3) hydrophobicity around the copper atom, (4) electrostatic effects due to the charges of the protein, and (5) hydrogen bonds toward the sulfur atom of the coordinated cysteine [5]. Among these factors, our main interest lies in getting a deeper insight into the consequences of different distortions on the redox potential.

Most proteins containing the T1 Cu site have four residues coordinated to the copper atom. The effect of modifications in the bond distance of the fourth residue on their low/medium redox potentials has been studied widely [6]. A debate about the consequences of these structural distortions and their origins [7–9] was started in the 1990s, and some authors considered them as crucial to redox potential tuning. When the distance of the Cu-fourth residue (Met or Gln) is elongated, an increment in redox potential is observed [4]. It has been hypothesized, and theoretically supported [10–12], that the three remaining residues in T1 Cu remain almost unchanged.

On the other hand, it was observed that laccases where methionine was substituted by hydrophobic residues such as Phe or Leu, which are unable to act as fourth ligands, exhibit the highest redox potentials (regulation due to the decrease in coordination number) [3]. Thus, the combination of a low coordination number and further distortions on the three-coordinated T1-Cu sites presents itself as an attractive strategy to raise redox potentials.

Two minima, very close in energy, were found from density functional theory (DFT) calculations on simplified models of the fourth-coordinated T1 Cu site when the potential energy surface was analyzed [11], and were correlated with an amyacin mutant [10] where two different colorations can be observed; the color changes from blue to green when the protein is cooled below 200 K. Equilibrium between the two minima, assisted by small distortions of the protein, has been suggested and, depending on the enzyme, one or another state is favored. This phenomenon was rationalized in terms of the differences in the orbital interaction of the Cu–S_{Cys} bond [4]. When the interaction is dominated by a π-overlap, the protein color is blue, whereas the color turns to green when the pseudo-σ overlap controls the interaction. This classification of interactions has been described previously [13]. Most of the proteins exhibit both types of interactions, to some extent, depending on the orientation of the $d_{x^2-y^2}$ copper orbital with regard to the residues of the first coordination sphere. Particularly, in the case of *Myceliophtora thermophila* laccase, the rotation of the orbital $d_{x^2-y^2}$, when some mutations are made, promotes a change in color of the active site from blue to green, presumably due to an increase of the pseudo-σ interaction, with a concomitant decrease in the π-overlap in the Cu–S bond [14].

Taking into account a model of a three-coordinated T1 Cu site (corresponding to laccases with the highest redox potentials), and using the DFT framework, systematic modifications of geometrical parameters (distances and angles) on the coordination sphere of the active site were carried out in the present study, in order to simulate possible distortions that might result in higher redox potentials. The effect of these geometrical distortions on the electron affinity (directly related to redox potentials) was evaluated, with special emphasis on two minima characterized from the potential energy surface, linkable to an equilibrium between two states of three-coordinated copper sites.

Methods

Validation

In order to start with a good quality description of the T1 Cu site embedded in laccases, a prior validation of the theoretical methods was made on three different copper models with structural similarities to T1 Cu (see Geometric validation in the supporting information). The crystallographic structures of the chosen models available in the literature [15–17] were taken as a reference for geometrical comparisons. Among the functionals M05, BP86, B3LYP, and PBE0, available in the DFT framework of the Jaguar 7.0 program [18], the hybrid functional PBE0 [19, 20] produced the best results and was selected for further calculations (maximum deviation of 0.09 Å in the copper–ligand distances compared to crystallographic distances).

The basis set, LACVP** [21, 22] with polarized functions on all atoms was used. This is a 6-31G basis set that takes into account effective core potentials (ECPs) generated to replace the innermost core electrons for third-row (K–Cu), incorporating in this way the relativistic effects of heavy atoms.

Since the property under study is the redox potential, the chosen functional (PBE0) was evaluated on three copper complexes, mimics of the T1 Cu site (see Redox validation in the supporting information), whose redox potentials were reported in the literature [23, 24]. The PBE0 functional gives redox potential values with an average deviation of 150 mV (3.5 kcal) from experimental data. These values are within the range of the DFT redox calculation error [25].

T1 Cu model under study and methodology

One of the laccases with higher redox potentials is that from *Trametes versicolor* [3, 26]; the crystal structure of *T. versicolor* laccase deposited in the Protein Data Bank (PDB ID: 1GYC). The T1 Cu of *T. versicolor* laccase is surrounded by two histidine and one cysteine residues. In

order to systematically explore the effect of geometrical distortions (in distances and angles) on the electron affinity of the T1 Cu site, a reduced model of *T. versicolor* laccase was chosen, including two methylimidazole groups and one methylthiolate, all directly coordinated to Cu (II) (Fig. 1).

Full geometry optimization of the T1 Cu model (Cu (II), multiplicity 2) was carried out at PBE0/LACVP** level (within unrestricted formalism), and the structural deviation of the active site with regard to the complete crystallographic structure was evaluated (see Results and discussion). The full optimized T1 Cu model was used as reference for further calculations.

From the fully optimized structures of T1 Cu (Cu (II), multiplicity 2), distances A, B, and C, angles α, δ, and dihedrals θ and ω were systematically modified, fixing each one in turn and optimizing the rest of the molecule, obtaining total energies for each specific modification. To calculate the electron affinities, total energies of Cu (I) counterparts were obtained by single point calculations of each structure with the corresponding modification.

Since the geometrical restrictions proposed here do not allow a complete relaxation of the structures, the electron affinities are vertical ones. Taking into account the thermodynamic cycle of Fig. 2 [27] and the equations shown below, the redox potentials were estimated from vertical calculations of electron affinities. The reduction properties of the Cu (II) open-shell system under the unrestricted formalism are related to an unoccupied molecular orbital (labeled as β-LUMO) that was used for a qualitative description of orbitals rearrangement.

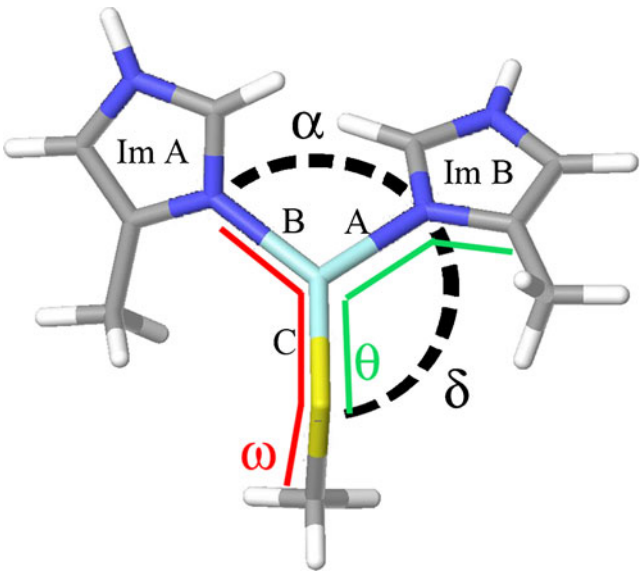

Fig. 1 T1 Cu model. Labels correspond to distances *A*, *B*, and *C*; angles α and δ, and dihedral angles ω and θ

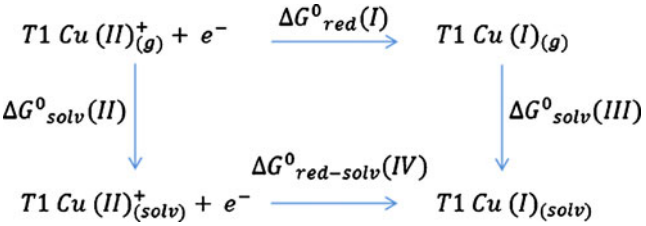

Fig. 2 Thermodynamic cycle

The global ΔG in solution ($\Delta G_{\text{red-solv}}{}^{0}$(IV)) can be expressed as follows:

$$\Delta G^{0}_{\text{red}-\text{solv}}(\text{IV}) = \Delta G^{0}_{\text{red}}(\text{I}) + \Delta G^{0}_{\text{solv}}(\text{III}) - \Delta G^{0}_{\text{solv}}(\text{II}) \quad (1)$$

Once the free energy change in solution is defined, the absolute redox potential E^0 can be determined as:

$$\text{E}^{0} = -\Delta G^{0}_{\text{red}}(\text{I})/\text{nF} - \Delta G^{0}_{\text{solv}}(\text{III})/\text{nF} + \Delta G^{0}_{\text{solv}}(\text{II})/\text{nF} \quad (2)$$

Where *n* is the number of transferred electrons and F is the Faraday constant.

The redox potential might be defined through the electron affinity in gas phase by separation of terms, [$\Delta G_{\text{red}}{}^{0}$(I)] and the difference in solvation energies of the involved species [$\Delta G_{\text{solv}}{}^{0}$(II)−$\Delta G_{\text{solv}}{}^{0}$(III)]; thus, from the thermodynamic cycle, the electron affinity of T1 Cu $(\text{II})_{(g)}{}^{+}$ is calculated as the energy of T1 Cu $(\text{II})_{(g)}{}^{+}$ minus the energy of T1 Cu $(\text{I})_{(g)}$, both in gas phase. The $\Delta G_{\text{red}}{}^{0}$(I) value is estimated as the energy difference between T1 Cu $(\text{I})_{(g)}$ and T1 Cu $(\text{II})_{(g)}{}^{+}$; therefore the electron affinity of T1 Cu $(\text{II})_{(g)}{}^{+}$ is equal to $-\Delta G_{\text{red}}{}^{0}$(I). In this way, it is possible to establish a tendency in redox potentials through electron affinity only.

In the particular case of multicopper oxidases, there is a very small geometric reorganization of the T1 Cu site upon reduction to Cu (I) [28], according to crystallographic studies. Thus, strictly speaking, in the environment of the protein the use of ΔE values in the thermodynamic cycle would be valid (since almost no entropic contributions by reorganization are involved). Even though this approximation holds in the context of the protein and not in the small model of T1 Cu site, it can still be applied if it is considered that the geometrical distortions tested in the small model to enhance the redox potential are meant to be projected into the protein context. This approximation allows vertical electron affinities to be related to redox potentials. Therefore, ΔG values were replaced by ΔE values in the thermodynamic cycle.

Even though the most significant solvation energy is that of protein solvation (which is considered as constant), it is usually considered that the T1 Cu site is embedded in an environment with a certain dielectric constant of about 8 [29] (mostly hydrophobic); therefore, calculations in cyclohexane, tetrahydrofuran, and water were carried out

for distorted structures of the Cu (I)/Cu (II) model under the Poisson-Boltzmann solvation scheme [30, 31] and their redox potential was calculated with the aim of evaluating the possible effect of solvation on redox potential.

It has been pointed out that the solvation effects out of the coordination sphere of active sites play an important role in redox potential calculations. For most small complexes in solution, a reliable description can be obtained by means of solvation energy calculations using a continuum model that leaves aside parameters such as explicit charges, dipole moments and hydrogen bonds [32]. Some other approximations that include such parameters are: (1) QM/MM (quantum mechanics/ molecular mechanics) calculations, which explicitly take into account charges and hydrogen bonds from the protein at lower level of theory [33]; and (2) PDLD (protein dipoles langevin dipoles), considering dipole moments and charges [34]. Beyond the method chosen, the important issue is to be aware of the limitations of every model and the conclusions that can be drawn.

Results and discussion

After full optimization of the T1 Cu model chosen in the present study, distances Cu–S, Cu–$N_{His(ImA)}$, and Cu–$N_{His(ImB)}$ (Fig. 1) are generally longer than crystallographic ones, but differing only by 0.011, 0.032, and 0.012 Å, respectively. According to these results, the protein environment apparently does not exert a significant strain on the T1 Cu site.

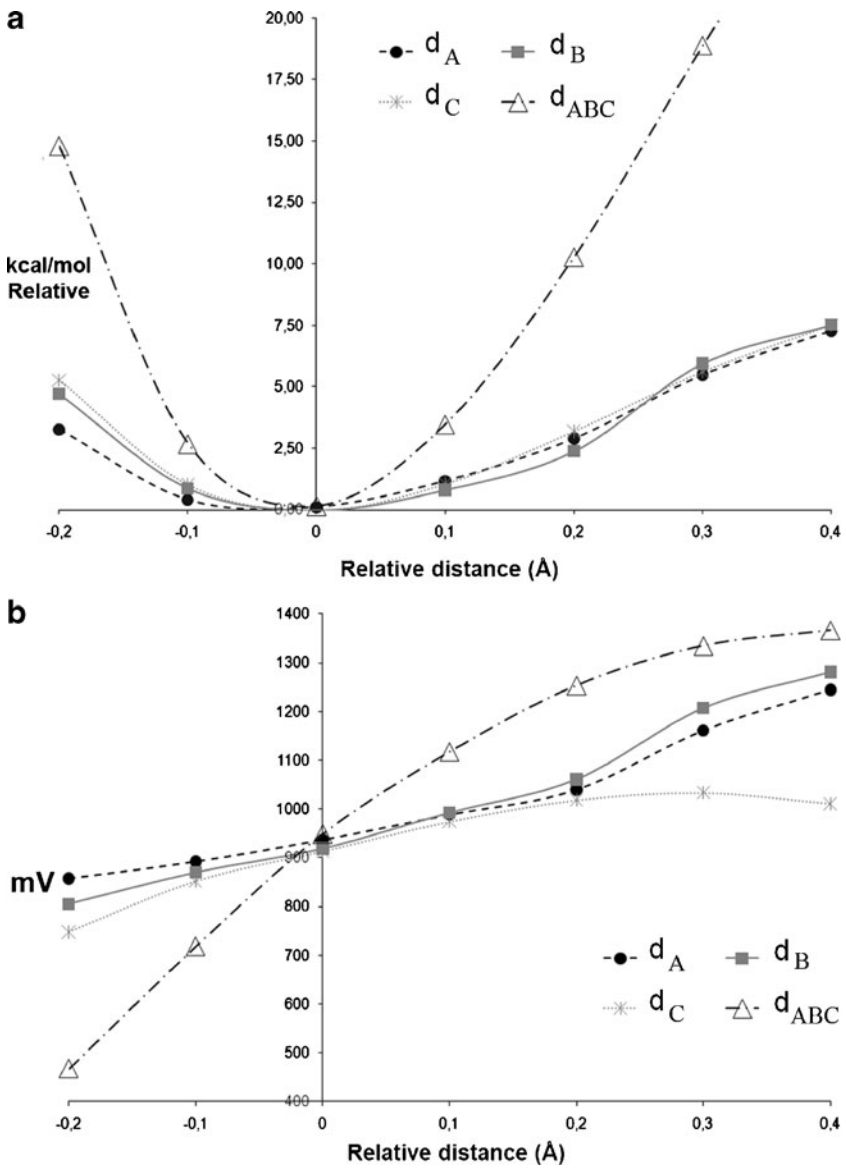

Fig. 3 Systematic modification of distances *A* (d_A), *B* (d_B), and *C* (d_C). d_{ABC} corresponds to the synchronized modification of these three distances. The zero value in the *x*-axis corresponds to the distances of the fully optimized structure. **a** Relative energies versus distorted distances. **b** Vertical electron affinities versus distorted distances

Systematic tension in bond distances

Distances A, B, and C (Fig. 3) were individually modified (shortened and increased) from −0.2 to 0.4 Å in increments of 0.1 Å. Optimization of the structures with the corresponding fixed distance were carried out and the relative energies of the complexes, as well as their vertical electron affinities (values in mV and referenced to NHE), were computed. Another series in which distances A, B, and C were synchronically modified was also generated, computing both relative energies and vertical electron affinities.

It can be seen from Fig. 3 that any tension resulting in a contraction of the distances would imply destabilization in the energy of the complex and a decrease of electron affinities.

When distances A and B (involving imidazole rings) are increased, the electron affinities also increase progressively and, even though the complex loses stability, it does so to a moderate extent. Modification of the Cu–S distance (C) resulted in a marginal increment of electron affinity, and the synchronized movement of distances (d_{ABC}) produced the highest destabilization of the complex. However, separation of the ligands from copper, which emulates the scenario where a decrease of coordination number might occur, produces an important increment of the electron affinity. Thus, considering both effects, those tensions that increase the Cu–ligand distances might produce only a modest increment of redox potentials.

The energy of the redox active molecular orbital, labeled as β-LUMO, follows the same tendency as the vertical affinities (as shown in Fig. 4), since both parameters are related directly to the redox potentials of the T1 Cu site model; therefore, changes on this molecular orbital can be used to describe redox potential variations. This pattern was also observed in all the geometrical distortions discussed here.

Systematic distortions in angles

Next, the angles α (N–Cu–N) and δ (N–Cu–S) were independently modified from 90 to 180°, in increments of 10° and the structures were optimized with the corresponding fixed

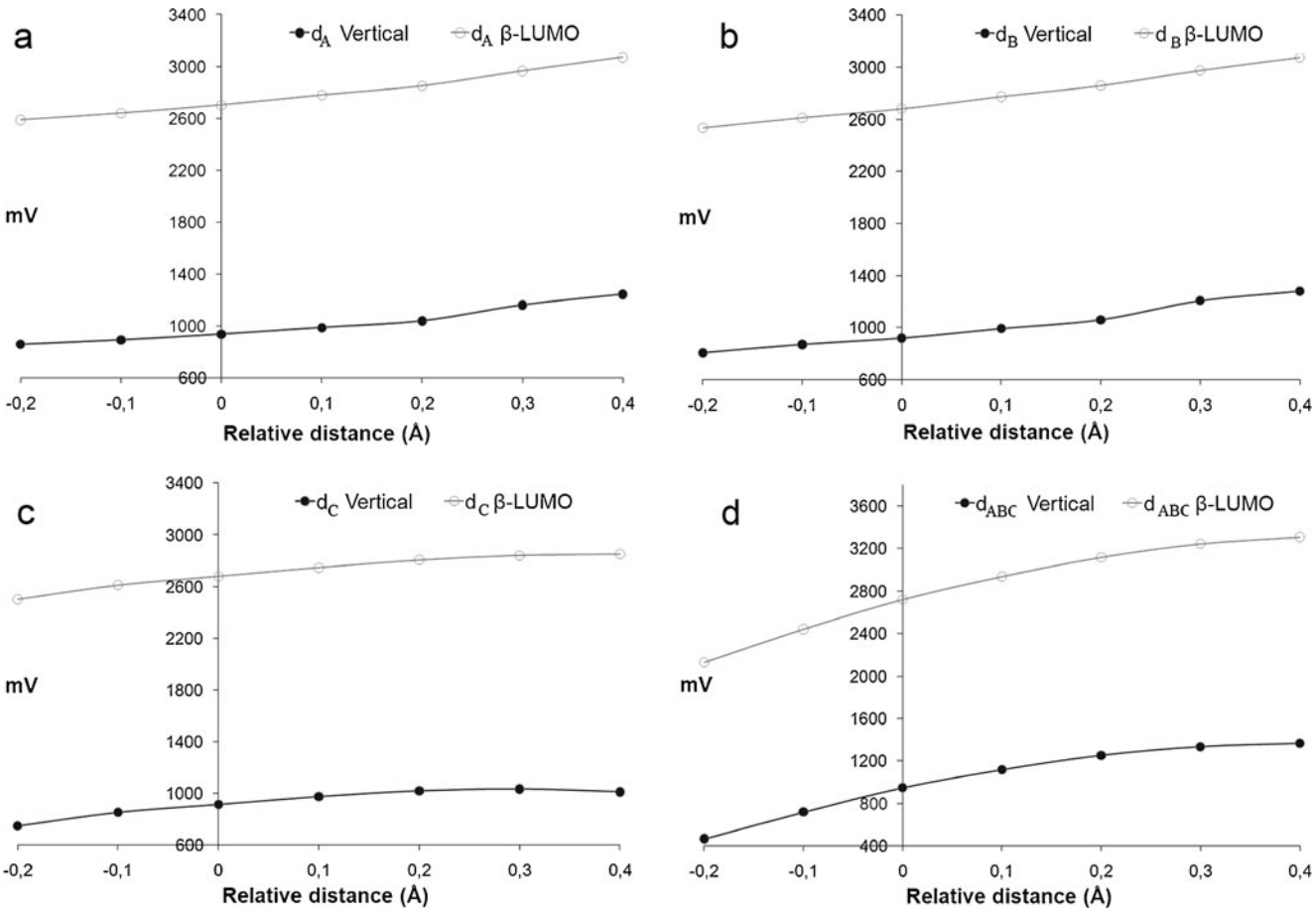

Fig. 4 Vertical electron affinities and β-LUMO energies during systematic modification of distances. **a** *A*, d_A; **b** *B*, d_B; **c** *C*, d_C; and **d** the synchronized distances *A*, *B*, and *C*. The zero value in the *x*-axis corresponds to the distances of the fully optimized structure

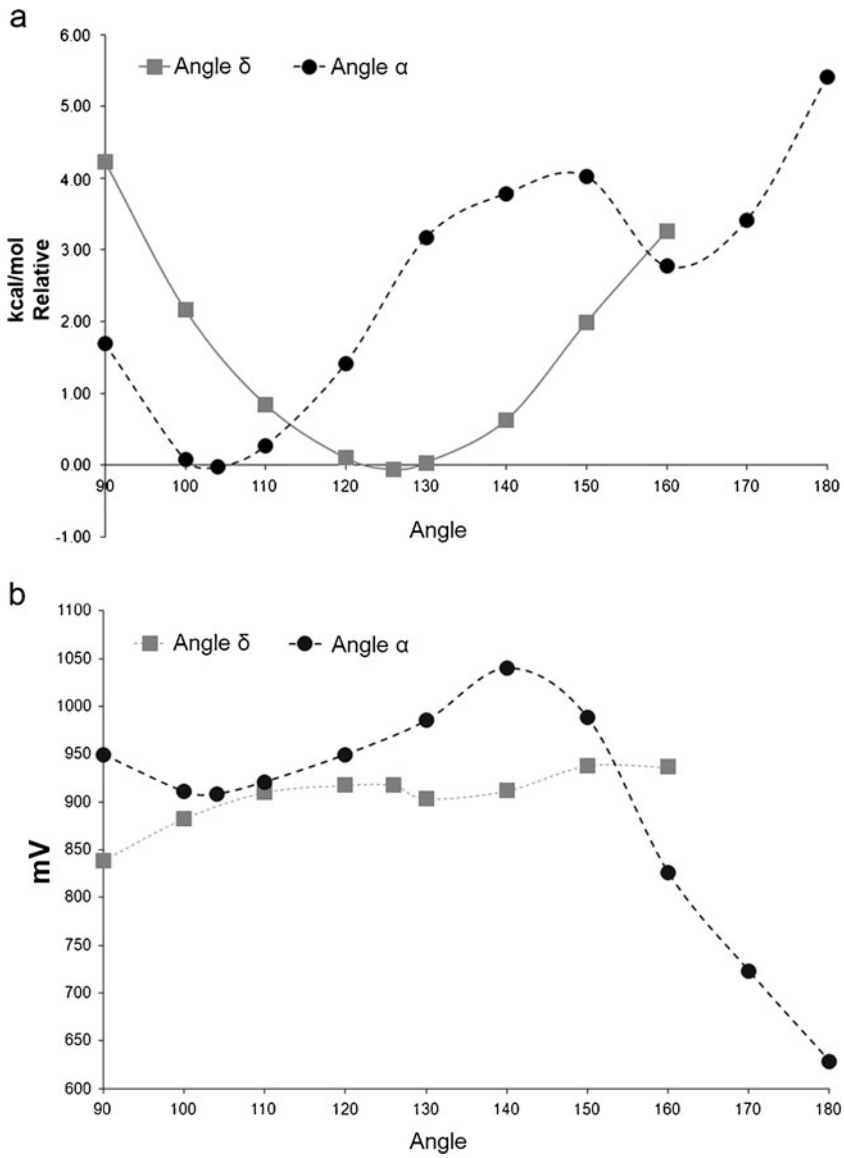

Fig. 5 Systematic modification of angles α (N_{ImA}–Cu–N_{ImB}) and δ (S–Cu–N_{ImA}). **a** Relative energies versus distorted angles. **b** Vertical electron affinities versus distorted angles

angle. The angles α=104° and δ=126° match with the crystallographic structure and were also considered (see Fig. 5).

As observed, the modification of angles gives rise to a very different energy pattern since additional effects, such as electronic repulsion and steric hindrance, are now involved. From the modification of angle δ, the minimum energy of the complex in the curve corresponds to the crystallographic structure. Throughout the modifications, only a small increment in the vertical electron affinity (less than 40 mV) is observed, whereas the modification of angle α produces an increment of around 120 mV, with similar complex destabilization. An increase in the angle α from 140° to 180° prevents the π interaction between copper and sulfur by steric hindrance. This effect acts in favor of the anti-bonding β-LUMO stabilization at angles of 140° and 150°, where the participation of only one of the imidazole rings via the nitrogen, and the thiolate group via a pseudo-σ overlap is observed. This effect changes from 160° to 180° where the above scenario remains but, in addition, the overlap of the second imidazole increases, destabilizing the β-LUMO (Fig. 6).

So far a single modification of the Cu–N distance provides the best compromise between destabilization of the complex and the increment of the vertical electron affinity.

Systematic distortions in dihedral angles

The two planes involved in the dihedral angle S–Cu–N_{ImA}–C_{ImA} (θ) were defined by N_{ImA}–N_{ImB}–S–Cu atoms (first plane) and the atoms of imidazole A (second plane); see Fig. 1. Once the planes were defined, the dihedral θ was modified from 0 to 350° in increments of 10°. In this case, as imidazole A was rotating, imidazole B compensated for

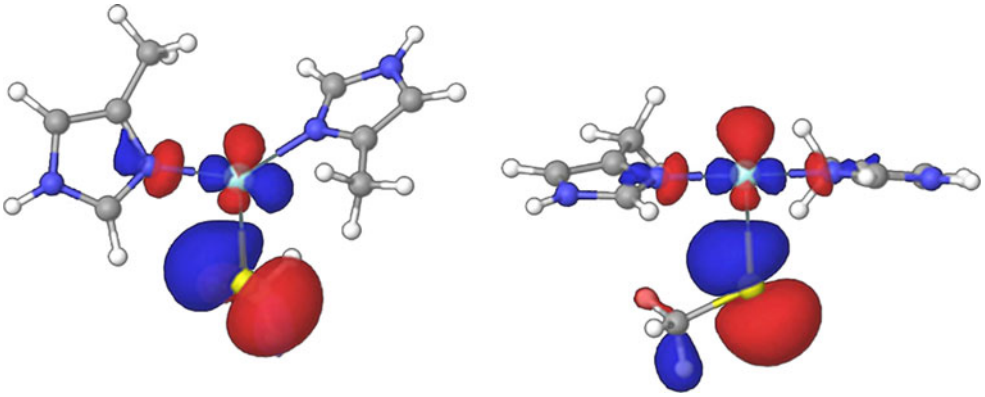

Fig. 6 Graphical representation of β-LUMO. *Left* Angle α= 140° *right* angle α=180°

this rotation (see Fig. 7). Hence, this rotation causes a cancellation of any possible electronic rearrangement.

When the relative energies and vertical electron affinities are plotted, one can see small changes in both destabilization energy and vertical electron affinity, with a periodic behavior of both graphs (Fig. 8).

The leading role of the Cu–S interaction in the modulation of the T1 Cu redox potential has been recognized to be as a major contributor to the stabilization of the oxidized site of blue proteins [35]. To evaluate the effect of modification of the dihedral angle involving this interaction, the $C_{methylthiolate}$–S–Cu–N_{ImA} dihedral angle (ω in Fig. 1) was rotated from 0° to 270° in increments of 10°, around the plane formed by the N_{ImA}–N_{ImB}–S–Cu atoms. The relative energy of the complex and the vertical electron affinity patterns are shown in Fig. 9. It can be seen from the graph that the best trade-off between the increment of vertical electron affinity and complex destabilization is achieved with this distortion.

There is a minimum in the energy of the complex at 0° (or 180°) that is related to a change in the imidazole ring conformations. A small increment from 0° to 10° in ω produces a change of more than 40° in the angle N_{ImA}–Cu–N_{ImB}. This result is rationalized below in terms of molecular orbitals.

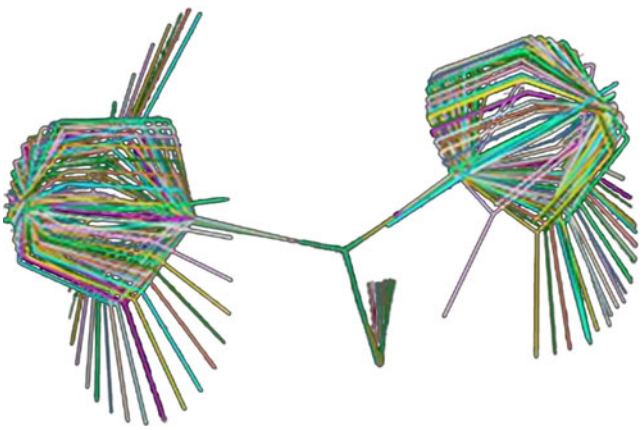

Fig. 7 Superposition of structures generated by rotation of the dihedral angle θ

The most significant increment in the vertical electron affinity is observed in conformations with ω=10° and −10°, which would correspond to a theoretical increment in redox potential of 390 mV. It is important to mention that other kinds of modification, like the presence or absence of a fourth ligand, would modify the redox potential only by 80–120 mV [4].

To explain the singular pattern of the vertical electron affinity as the dihedral angle ω is modified, the changes in the β-LUMO were represented by three key conformations selected from Fig. 9: ω=0°, 20°, and 90° (Fig. 10).

Starting with the structure where ω=90°, it is observed that the $d_{x^2-y^2}$ orbital of copper, one p orbital of sulfur, and two σ-lobes from the imidazole rings contribute to β-LUMO. When the dihedral ω is modified, the p orbital of sulfur is rotated around the Cu–S axis (see Fig. 10, lateral view, 20° configuration). The copper $d_{x^2-y^2}$ orbital follows the movement of the p orbital of sulfur to maximize the overlap between them, sacrificing the interaction between copper and the imidazole rings. The smaller overlap results in greater stability of β-LUMO and, as the dihedral ω is rotated, the β-LUMO is stabilized due to a smaller interaction with orbitals from the imidazole rings.

For ω=20°, the $d_{x^2-y^2}$ orbital from copper is out of plane by 30°, diminishing all σ interactions (Fig. 10). When the rotation is 0°, there is a notable change in the orbital disposition; the orbital $d_{x^2-y^2}$ does not contribute to β-LUMO and instead the d_{xy} orbital of copper does; this result can be interpreted also as a 45° rotation of the $d_{x^2-y^2}$ orbital around the z axis. This conformation allows the imidazole rings to interact with distal lobes of the d orbital of copper. Finally, the original p orbital of sulfur remains perpendicular to the plane of ligands due to the change in orientation, leaving the other p orbital of sulfur to interact by a single lobe with copper. This conformational change with its concomitant electronic rearrangement explains the

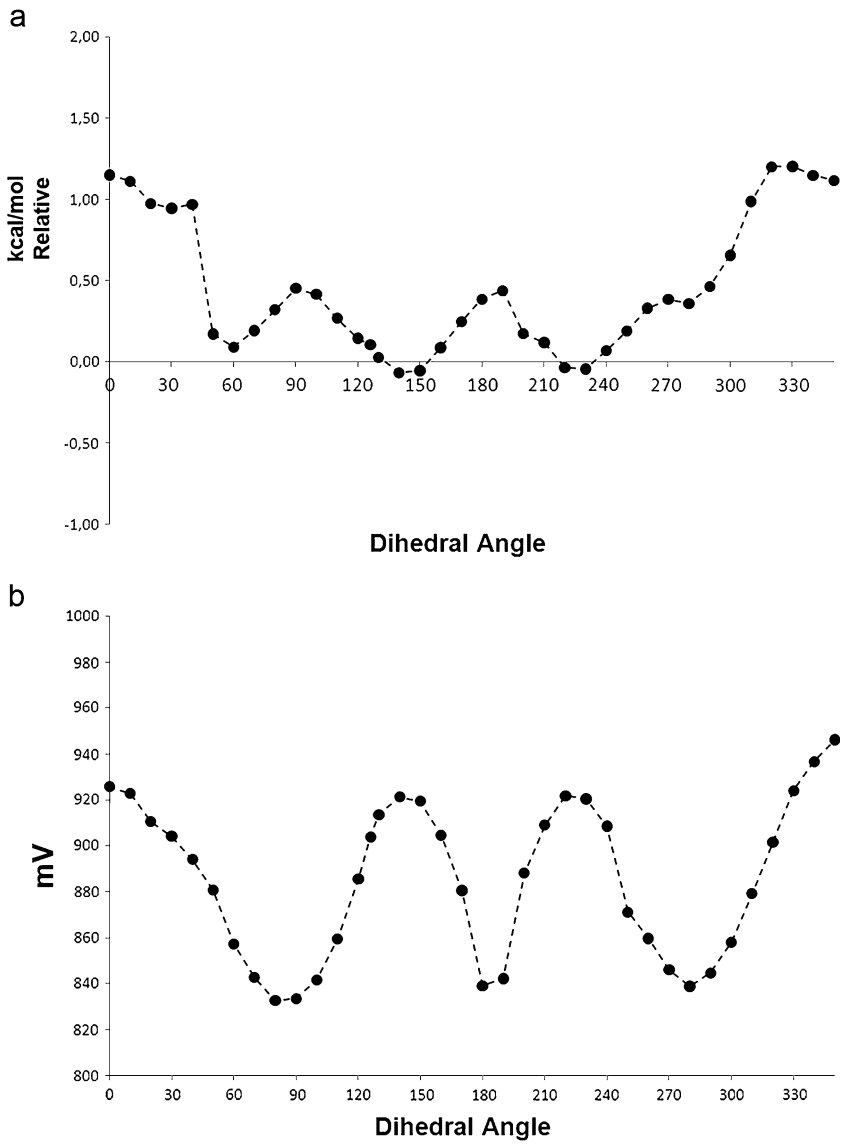

Fig. 8 Systematic modification of dihedral angle θ (S–Cu–N_{ImA}–C_{ImA}). **a** Relative energies versus distorted dihedral angle, **b** vertical electron affinities versus distorted dihedral angle

abrupt change in energy of both the complex and the β-LUMO.

Along the modification of the dihedral angle ω, two minima are generated, one in ω=90° (minimum 1) and the other in ω=0° (minimum 2). These conformations were fully optimized, and frequency calculations were carried out to verify the order of each saddle point. After optimization, the dihedral ω remains almost the same (95.3° and 0°, respectively). An energy difference of 1.7 kcal mol^{-1} between them was found, being more stable the minimum 1. The minimum 1 conformation virtually coincides with many of the crystallographic structures of high potential laccases with three-coordinated T1 Cu sites. The transition state between these minima was calculated as an energy barrier of 4.6 kcal. According to a Boltzmann distribution calculation, 6% of the T1 Cu site exists in state 2 at room temperature; however, the protein seems to restrict the T1 Cu site to constantly adopt the conformation of minimum 1 over minimum 2. This is supported by the fact that no significant pseudo-σ interaction has been identified spectroscopically in high redox potential laccases [4], suggesting that the proteins might exert restrictions over the T1 Cu site, and that these restrictions coincide with the minimum 1.

It is important to establish that the β-LUMO in minimum 1 possesses a π-character in the Cu–S interaction, whereas in minimum 2 a pseudo-σ character prevails.

These interactions define the spectroscopic properties of the complexes. Earlier experimental studies attributed the T1 Cu site color change to an adjustment in the Cu–S interaction through the presence of a fourth ligand. According to the results obtained in the present study, the same color change can occur in the absence of a fourth ligand (see Supporting information).

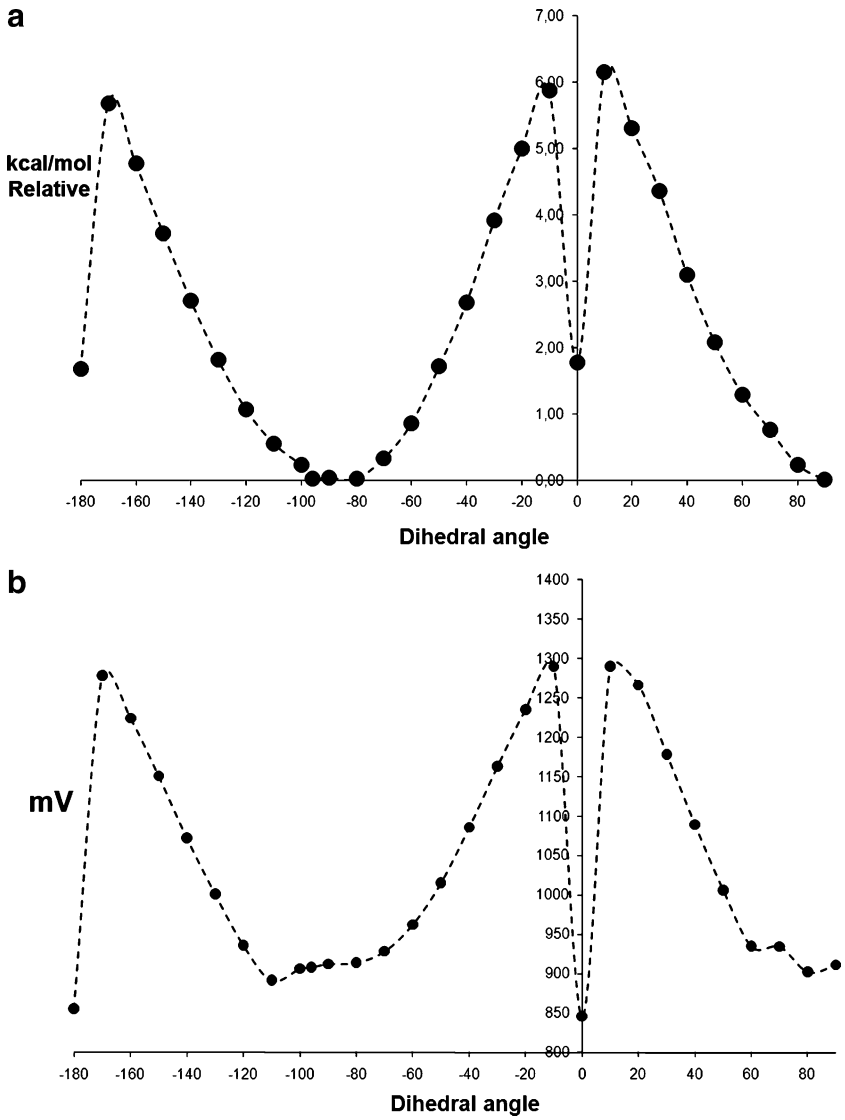

Fig. 9 Systematic modification of $C_{methylthiolate}$–S–Cu–N_{ImA} dihedral angle ω. **a** Relative energies versus distorted dihedral angle, **b** vertical electron affinities versus distorted dihedral angle

Solvation effects during systematic distortions

To evaluate the solvation effect on the redox potential of the T1 Cu site during systematic distortions, the modification of the dihedral angle ω (from 0° to 90°) was considered in three different solvents (cyclohexane, tetrahydrofuran, and water), following the thermodynamic cycle from Fig. 2. Redox potential values were estimated and are shown in Fig. 11.

It can be seen from Fig. 11 that, even though the net values of redox potential change depend on the dielectric constant of each solvent, the tendency remains almost the same. The dielectric constant inside the protein is about 8 [28], which is closer to the dielectric constant of cyclohexane (7.6). Thus, according to these results, it can be concluded that the solvation energy has little influence on any of the tendencies observed when geometric distortions are made.

Conclusions

A model of three-coordinated T1 Cu site from *T. versicolor* was used to carry out geometric distortions in a systematic fashion to evaluate their effect on redox potential modulation. Distortions in the Cu–N distance produced only a modest tuning of redox potential.

The best approach to increase redox potential was by distortion of the dihedral angle ω, rationalized as a decrease in the overlap of imidazole orbitals in the redox-active molecular orbital (β-LUMO).

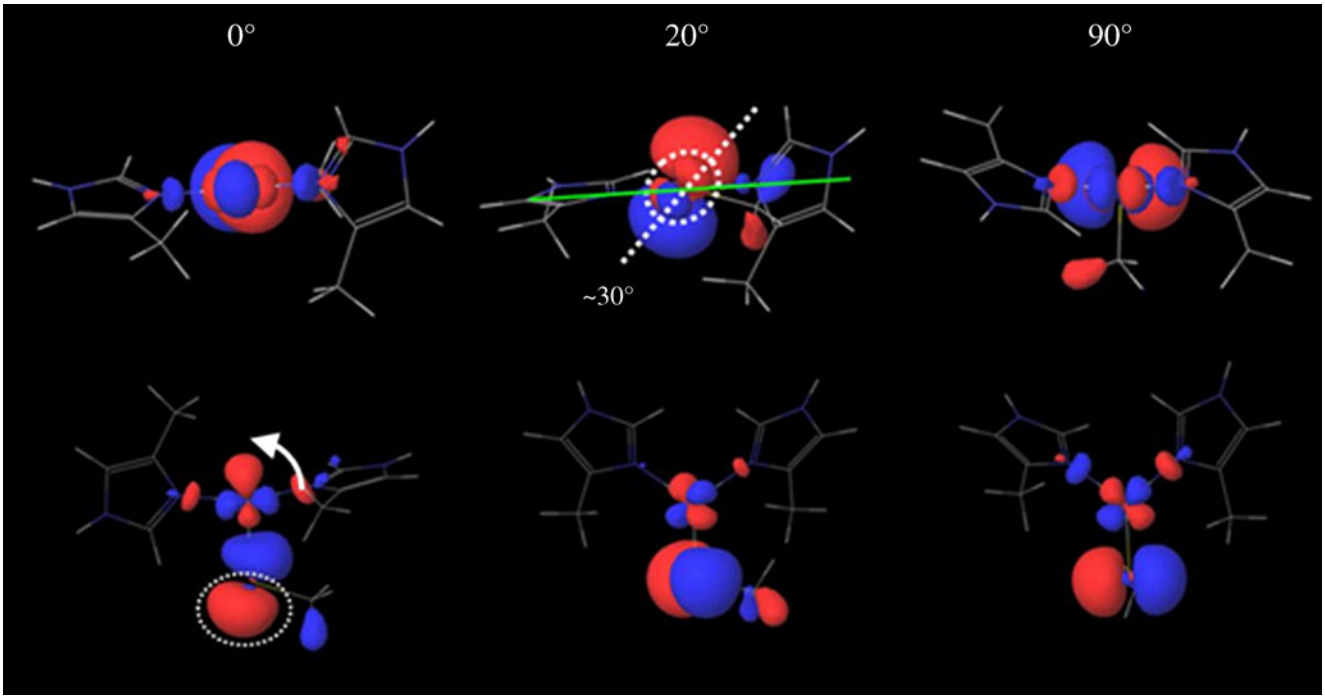

Fig. 10 β-LUMO representation in conformation with ω=0°, 20°, and 90°. *Top* Lateral view, *bottom* upper view

Another important result was the characterization of two minima, and the transition state between them for the first coordination sphere of T1 Cu site. According to the energy barrier between these two structures, they might be in equilibrium at room temperature in the absence of external restrictions (protein tensions). Hence, it is proposed that the laccase of *T. versicolor* restricts the T1 Cu site to adopt just the minimum 1 state.

The two minima described above can be distinguished clearly in terms of molecular orbitals. For minimum 1, the Cu–S interaction can be described as predominantly π in nature, whereas the minimum 2 is better described as a pseudo-σ interaction.

It was shown that the T1 Cu site redox potential during distortions follows the same pattern either in vacuum or in solution.

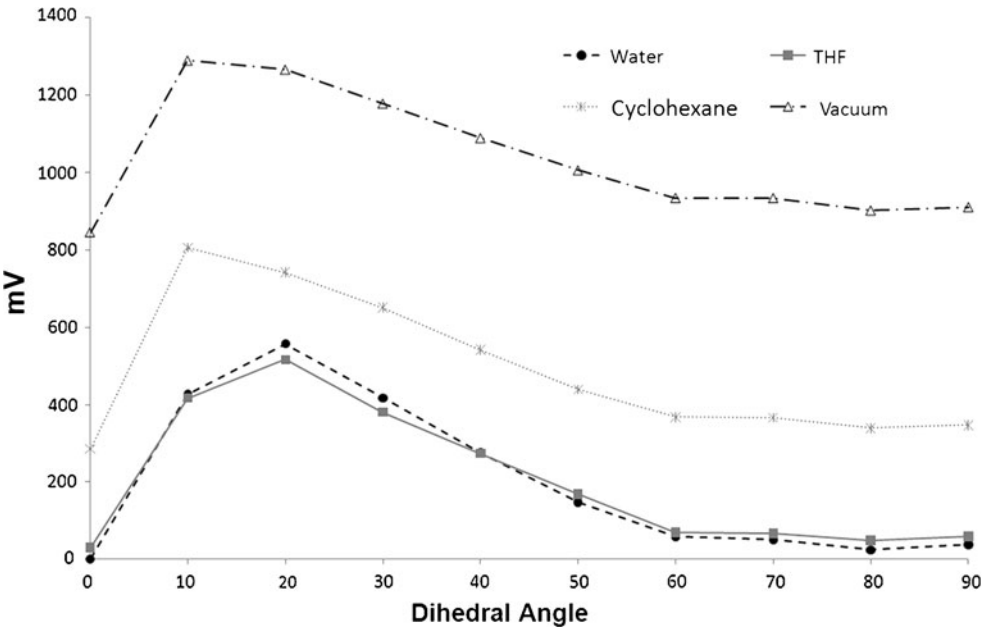

Fig. 11 Redox potential values of the T1 Cu model during the dihedral angle (ω) distortion in three different solvents (water, tetrahydrofuran and cyclohexane)

Acknowledgments We acknowledge the support of the Dirección General de Servicios de Cómputo Académico, from Universidad Nacional Autónoma de México, for the use of the supercomputer KanBalam and the Consejo Nacional de Ciencia y Tecnología for a doctoral scholarship. We also thank L.I. Victor Manuel Gómez for his valuable technical support.

References

1. Palmer AE, Randall DW, Xu F, Solomon EI (1999) Spectroscopic studies and electronic structure description of the high potential type 1 copper site in fungal laccase: insight into the effect of the axial ligand. J Am Chem Soc 121:7138–7149. doi:10.1021/ja991087v
2. Solomon EI, Sundaram UM, Machonkin TE (1996) Multicopper oxidases and oxygenases. Chem Rev 96:2563–2605. doi:10.1021/cr950046o
3. Shleev SV, Morozova OV, Nikitina OV, Gorshina ES, Rusinova TV, Serezhenkov VA, Burbaev DS, Gazaryan IG, Yaropolov AI (2004) Comparison of physico-chemical characteristics of four laccases from different basidiomycetes. Biochimie 86:693–703. doi:10.1016/j.biochi.2004.08.005
4. Solomon EI, Szilagyi RK, George SD, Basumallick L (2004) Electronic structures of metal sites in proteins and models: contributions to function in blue copper proteins. Chem Rev 104:419–458. doi:10.1021/cr0206317
5. Li H, Webb SP, Ivanic J, Jensen JH (2004) Determinants of the relative reduction potentials of type1-copper sites in proteins. J Am Chem Soc 126:8010–8019. doi:10.1021/ja049345y
6. Christensson A, Dimcheva N, Ferapontova E, Gorton L, Ruzgas T, Stoica L, Shleev S, Haltrich YAD, Thorneley R, Aust S (2004) Direct electron transfer between ligninolytic redox enzymes and electrodes. Electroanalysis 16:1074–1092. doi:10.1002/elan.200403004
7. Ryde U, Olsson MHM, Pierloot K, Roos BO (1996) The cupric geometry of blue copper proteins is not strained. J Mol Biol 261:586–596. doi:10.1006/jmbi.1996.0484
8. Malstrom BG (1994) Rack-induced bonding in blue-copper proteins. Eur J Biochem 223:711–718. doi:10.1111/j.1432-1033.1994.tb19044.x
9. Williams RJP (1995) Energised (entatic) states of groups and of secondary structures in proteins and metalloproteins. Eur J Biochem 234:363–381. doi:10.1111/j.1432-1033.1995.363_b.x
10. Comba P, Müller V, Remenyi RJ (2004) Interpretation of the temperature-dependent color of blue copper protein mutants. Inorg Biochem 98:896–902. doi:10.1016/j.jinorgbio.2003.12.004
11. Ryde U, Olsson MHM (1999) The influence of axial ligands on the reduction potential of blue copper proteins. J Biol Inorg Chem 4:654–663. doi:10.1007/s007750050389
12. Pavelka M, Burda JV (2008) Computational study of redox active centres of blue copper proteins: a computational DFT study. Mol Phys 106:2733–2748. doi:10.1080/00268970802672684
13. Holm H, Kennepohl P, Solomon EI (1996) Structural and functional aspects of metal sites in biology. Chem Rev 96:2239–2314. doi:10.1021/cr9500390
14. Palmer AE, Szilagyi RK, Cherry JR, Jones A, Xu F, Solomon EI (2003) Spectroscopic characterization of the Leu513His variant of fungal laccase: effect of increased axial ligand interaction on the geometric and electronic structure of the type 1 Cu site. Inorg Chem 42:4006–4017. doi:10.1021/ic026099n
15. Karlin KD, Dahlstrom PL, Hyde JR, Zubieta J (1980) Structural comparison of Cu^{I} and Cu^{II} complexes displaying analogous N_2S_2 co-ordination; X-ray analysis of tetracoordinate [Cu(pma)]BPh_4 and pentaco-ordinate [Cu(pma)SO_4][pma=2-pyridylmethylbis-(2-ethylthioethyl)amine]. J Chem Soc Chem Commun 1980:906–908. doi:10.1039/C39800000906
16. Brines LM, Shearer J, Fender JK, Schweitzer D, Shoner SC, Barnhart D, Kaminsky W, Lovell S, Kovacs JA (2007) Periodic trends within a series of five-coordinate thiolate-ligated [MII (SMe2N4(tren))]+(M) Mn, Fe, Co, Ni, Cu, Zn) complexes, including a rare example of a stable CuII-thiolate. Inorg Chem 46:9267–9277. doi:10.1021/ic701433p
17. Cao Y, Zheng Q, Chen C, Hu H, Huang Z (2004) Synthesis of a novel three-coordinate copper(I) complex: a structural mimic of the reduced form of type 1 site in copper protein. Inorg Chim Acta 357:316–320. doi:10.1016/S0020-1693(03)00469-9
18. Jaguar, version 7.0 (2007) Schrödinger, New York
19. Adamo C, Barone V (1999) Toward reliable density functional methods without adjustable parameters: the PBE0 model. J Chem Phys 110:6158–6170. doi:10.1063/1.3454734
20. Vetere V, Adamo C, Maldivi P (2000) Performance of the 'parameter free' PBE0 functional for the modeling of molecular properties of heavy metals. Chem Phys Lett 325:99–105. doi:10.1016/S0009-2614(00)00657-6
21. Hay PJ, Wadt WR (1985) Ab initio effective core potentials for molecular calculations. Potentials for the transition metal atoms Sc to Hg. J Chem Phys 82:270–283. doi:10.1063/1.448799
22. Hay PJ, Wadt WR (1985) Ab initio effective core potentials for molecular calculations. Potentials for K to Au including the outermost core orbitals. J Chem Phys 82:299–310. doi:10.1063/1.448975
23. Holland PL, Tolman WB (1999) Three-coordinate Cu (II) complexes: structural models of trigonal-planar type 1 copper protein active sites. J Am Chem Soc 121:7270–7271. doi:10.1021/ja991533e
24. Holland PL, Tolman WB (2000) A structural model of the type 1 copper protein active site: N_2S(thiolate)S(thioether) ligation in a Cu (II) complex. J Am Chem Soc 122:6331–6332. doi:10.1021/ja001328v
25. Uudsemma M, Tamm T (2003) Density-functional theory calculations of aqueous redox potentials of fourth-period transition metals. J Phys Chem A 107:9997–10003. doi:10.1021/jp0362741
26. Piontek K, Antorini M, Choinowski TJ (2002) Crystal structure of a laccase from the fungus *Trametes versicolor* at 1.90-Å resolution containing a full complement of coppers. Biol Chem 277:37663–37669. doi:10.1074/jbc.M204571200
27. Namazian M, Coote ML (2007) Accurate calculation of absolute one-electron redox potentials of some *para*-quinone derivatives in acetonitrile. J Phys Chem A 111:7227–7232. doi:10.1021/jp0725883
28. Hakulinen N, Kruus K, Koivula A, Rouvinen J (2006) A crystallographic and spectroscopic study on the effect of X-ray radiation on the crystal structure of *Melanocarpus albomyces* laccase. Biochim Biophys Acta 350:929–934. doi:10.1016/j.bbrc.2006.09.144
29. Datta SN, Sudhamsu J, Pandey A (2004) Theoretical determination of the standard reduction potential of plastocyanin in vitro. J Phys Chem B 108:8007–8016. doi:10.1021/jp0307452
30. Tannor DJ, Marten B, Murphy R, Friesner RA, Sitkoff D, Nicholls A, Ringnalda M, Goddard WA, Honig B (1994) Accurate first principles calculation of molecular charge distributions and solvation energies from ab initio quantum mechanics and continuum dielectric theory. J Am Chem Soc 116:11875–11882. doi:10.1021/ja00105a030
31. Marten B, Kim K, Cortis C, Friesner RA, Murphy RB, Ringnalda MN, Sitkoff D, Honig B (1996) New model for calculation of

solvation free energies: correction of self-consistent reaction field continuum dielectric theory for short-range hydrogen-bonding effects. J Phys Chem 100:11775–11788. doi:10.1021/jp953087x
32. Evans D (2008) One-electron and two-electrontransfer in electrochemistry and homogeneous solution reactions. Chem Rev 108:2113–2144. doi:10.1021/cr068066l
33. Olsson M, Hong G, Warshel A (2003) Frozen density functional free energy simulations of redox proteins: computational studies of the reduction potential of plastocyanin and rusticyanin. J Am Chem Soc 125:5025–5039. doi:10.1021/ja0212157
34. Stephens PJ, Jollie DR, Warshel A (1996) Protein control of redox potentials of iron sulfur proteins. Chem Rev 96:2491–2513. doi:10.1021/cr950045w
35. Kitajima N (1992) Synthetic approach to the structure and function of copper proteins. Adv Inorg Chem 39:1–77. doi:10.1016/S0898-8838(08)60258-5